13th International Symposium on Particle Image Velocimetry – ISPIV 2019
Munich, Germany, July 22-24, 2019

Pressure field calculation from streamline behavior in the flow through adjacent rectangular orifices

Yishak Yusuf, Shadi Ansari, and David S. Nobes*

University of Alberta, Department of Mechanical Engineering, Edmonton, Canada

* david.nobes@ualberta.ca

Abstract

The convergence phenomenon in the viscous flow entering an orifice contributes to the pressure loss in the system primarily due to flow acceleration. This zone can also be fundamentally characterized by the curvature of streamlines in the near-inlet region. The streamlines curvature, which increases with the distance from the centerline, is affected by the flow Reynolds number and the distance between the center axis and walls of the upstream. Prior works have shown that the streamline curvature increases as the Reynolds number increases. As the wall distance increases, however, it decreases the curvature in the streamlines highlighting the role of orifices spacing in flow scenarios where multiple orifices are present. In this study, particle shadowgraph velocimetry experiments are used to investigate the convergence phenomenon for the flow entering multiple orifices. The measured velocity field is used to calculate streamlines. The pressure gradients in the streamwise and spanwise directions are calculated along the streamlines by using the equations of motion in streamline coordinates. The results were compared with the case of a single orifice to show that the curvature of streamlines occurs closer to the orifice inlet when there are multiple orifices.

Background

For viscous flows entering rectangular orifice contractions, the streamlines in the near inlet region undergo significant curvature. This phenomenon is referred to as flow convergence and its underlying characteristic is the acceleration of the flow (Utsunomiya et al., 1993; Yusuf et al., 2018). As a result, inertial effects to dominate in the proximity of the centerline, while near-inlet regions that are close to the wall will be shear dominated (Oliveira et al., 2007). The resulting change in the localized velocity and pressure distributions lead to losses which may cause a number of undesired phenomena.

To comment on the length of the flow convergence region, the location where the velocity increase begins can be used (Grose, 1983) (Yusuf et al., 2019). Alternatively, it can also be inferred from the curvature property of the streamlines along the flow direction. This information regarding the length of the convergence region can ultimately be used to identify the extent of the resulting pressure loss. The relationship between the curvature of streamlines due to flow convergence and velocity transition has significant importance in identifying effects from changes in the flow or configuration of the orifice such as varying its aspect ratio or the presence of neighbor orifices.

In this study the streamline behavior is used to investigate the convergence phenomenon for a viscous flow through a rectangular orifices. The flow through a single orifice and three adjacent orifices will

be considered to compare the effect of wall distance and Re. The following section presents the theory regarding equations of motion in streamline coordinates. The experimentation part of the study will be presented next followed by a discussion of results and major conclusions.

Theory

In a prior work, the authors have investigated the modeling and pressure drop measurement of the viscous flow through rectangular orifices (Yusuf et al., 2017a; 2017b). It has been seen that the smaller of the two dimensions has a stronger influence on the pressure loss characteristics due to its direct effect on the flow blockage and hence, the curvature of streamlines of the converging flow. The flow convergence phenomena has been compared for creeping flows at Reynolds number in the range $0.01 \leq Re \leq 0.1$. The definition of Re uses the mean velocity through the orifice, $\bar{u}$, and the hydraulic diameter, D_h, as the velocity and length scales, respectively.

In the analysis, the model for the velocity transition in the convergence region included an empirical parameter, ϕ, which has been defined to represent the flow convergence phenomenon (Yusuf et al., 2019). The flow convergence parameter is expressed as:

$$\phi = \frac{\sqrt{\pi} \cdot Re}{4} \left[\frac{K - (1 - \alpha^2)}{\frac{2AR}{AR + 1}(1 - \alpha)} \right] \tag{1}$$

where K is the non-dimensional pressure loss coefficient, α is the ratio of the orifice area to that of the upstream section, AR is the orifice aspect ratio, AR. The loss coefficient,K, represents the ratio of the static pressure drop across the orifice, to the kinetic energy term, $\rho\bar{u}^2/2$, where ρ is the density of the fluid. The modeling that led to the above expression solved the Navier-Stokes equation in one dimension by assuming an asymptotic velocity transition from the far field to the region within the orifice, or form a region of parallel streamlines to parallel streamlines.

To develop a 2-dimensional relationship between the pressure loss characteristics and streamline curvature, a technique that combines streamline measurement with pressure calculations can be used (Yusuf et al., 2018). Calculation of the pressure gradients along the streamlines can be accomplished by writing the equations of motion in streamlines coordinates. The definition of this coordinate system is given in Figure 2 following (Sonin, 2010).

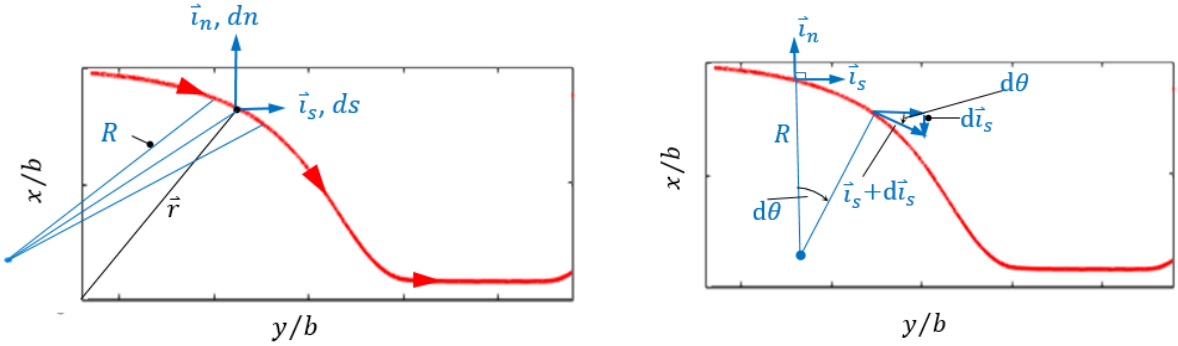

Figure 1: Definition of the streamline coordinate system (*after* Sonin, 2010)

By definition, the velocity vector is tangent to the streamline. A point on a streamlines is characterized in reference to the basis vectors shown in Fig.1 (a) along with the center and radius of curvature. A unit increase along the coordinate $d\vec{\imath}_s$ is obtained from the geometric construction shown Fig. 1(b). The equations of motion for an incompressible inviscid flow without including the effect from body forces can thus be written as:

$$-\frac{1}{\rho}\frac{\partial p}{\partial s} = \frac{\partial}{\partial s}\left(\frac{u^2}{2}\right) \tag{2}$$

$$-\frac{1}{\rho}\frac{\partial p}{\partial n} = \frac{u^2}{R} \tag{3}$$

where p is the pressure, u is the velocity, and R is the radius of curvature as defined in Fig. 1. The length scales s and n represent the coordinates in the streamwise and normal directions as shown in Figure 1. The equation in the streamwise direction, Eq. (2), gives Bernoulli's theorem which states that the total pressure along a streamline is constant. In Eq. (3), it is implied that the total pressure increases in the positive n-direction which points opposite to the center of curvature.

The curvature properties of the streamlines influence both pressure gradients in the s- and n-directions. The streamwise pressure drop is strongly associated with the velocity distribution along a streamline. Whereas the pressure gradient in the transverse direction has also a correlation with the curvature which can be seen through the presence of R in Eq. (3). Therefore, in the flow convergence region the resulting pressure is attributed not only to the flow acceleration but also to the curvature of the streamlines.

For a flow with a single orifice, it has been shown that the distance between the edge of the orifice and the wall of the upstream region affects the curvature properties (Yusuf et al., 2018). There can be a limit to this distance, D, beyond which the effects from the upstream wall become negligible. This information regarding the wall effect becomes important when referring to the spacing between neighboring orifices in the flow through multiple orifices rather than single.

In this study, particle shadowgraph velocimetry (PSV) experiments are used to investigate the flow through three adjacent orifices. The velocity measurement data is used to calculate the streamlines in the flow field. The results compare flows at $Re = 0.1$ and 1 in flow cells having a single and multiple orifices.

Experiment

The velocity field was measured by using the experimental setup shown in Figure 2. A common orifice width, $b = 1$mm, is maintained for all three orifices while the spacing, $D = 2.5b$. Experiments used glycerol (μ = 1.4138 Pa.s; ρ = 1260.8 kg/m^3 at 20 °C) at Re values of 0.1, and 1.

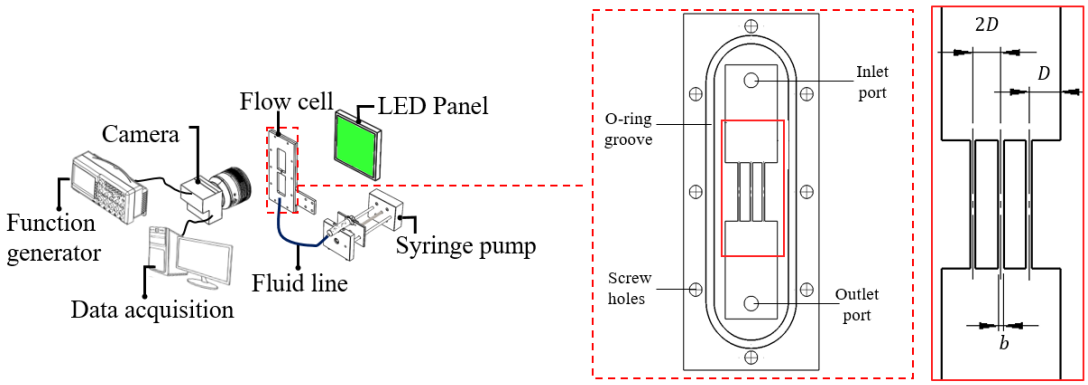

Figure 2: Schematics showing the setup and flow cell that will be used in the experiments

An example raw image captured by the experiment is shown in Figure 3(a). In order to track its motion, the fluid was seeded using 20 μm particles. In the plots shown, the flow is moving from left to right with gravity in the opposite direction. The origin of the coordinate system is placed at the entrance of the middle orifice as indicated in Fig. 3(a). For each *Re* considered, 650 numbers of images of the flow field were collected over 15 secs. The raw images were then processed as sequential frames to determine the velocity by a using commercial software (DaVis 10, LaVision GmbH). The velocity field was calculated using the cross-correlation of two sequential images with 2 passes having the window size of 32 × 32 with 50% overlap. The flow field in Fig. 3(b) shows the result from the processing for $Re = 0.1$. The velocity at all points is normalized by the maximum velocity which corresponds to the centerline velocity in the orifices. The axes labels indicate that the width of channel, b, was used to normalize the position vectors, x and y.

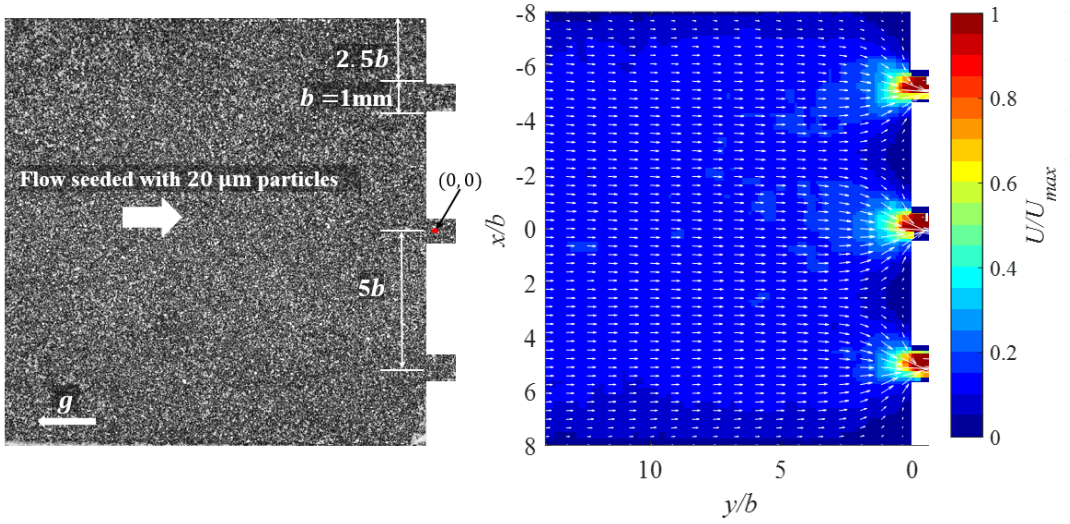

(a) (b)

Figure 3: (a) Raw image of the flow field, and (b) a colormap of the velocity vector field from processing of data for $Re = 0.1$

While the flow has a uniform velocity in the upstream region in Fig. 3(b), it starts to accelerate as it approaches the orifices inlets. The velocity vectors in the uniform region ($y/b > 4$) reflect this condition as they are parallel to the horizontal. At locations close to the walls, the magnitude of the vectors significantly decreases due to the no-slip boundary condition. In the convergence region,

however, the flow accelerates to increase to its maximum velocity inside the orifices. The flow in this region ($0 < y/b < 4$), is therefore highly dominated by inertial effects. Even though the bulk motion of the fluid remains in the same direction, its direction changes significantly and the angle between the velocity vectors and the horizontal is no longer zero.

The spatial information of this flow transition from conditions in the uniform flow zone to those in the convergence region can be better demonstrated by using the streamlines in the flow field. The properties of the streamlines can then be used to determine the length of the convergence region. The streamline curvature can be plotted as a function of the axial distance y/b to also infer the regions of maximum pressure gradient following the equations of motion in streamline coordinates described in the previous section. Once the streamlines are calculated, it is then possible to investigate the effect of flow and orifice geometry on the pressure distribution.

The velocity vector field data from processing of experimental data were further used to calculate the streamlines by using the method presented by (Yusuf et al., 2018). In brief, the calculation begins by specifying the starting point and using the velocity at that point the next position on the streamline can be calculated. This process is repeated until the specified number of points per streamline is reached. The x- and y-components of the velocity are recalled from the vector field data from the cross-correlation stage in the processing. The calculation of streamlines using this techniques has a number of advantages. This method provides total control over the properties of the streamlines plotted including the number of the streamlines, the spacing in between, and the number of points along each streamlines. Another significant advantage is that there is no need to specify the locations of solid walls nor set any boundary conditions thereof.

Results and Discussion

The plots shown in Fig. 4(a) and (b) show the streamlines calculated for the flow at $Re = 0.1$ through a single and multiple orifices, respectively. All the orifices having an equal width $b = 1$ mm. In Fig. 4(a), the wall distance is $D = 5$ which is also equal to the distances between the centerlines of the orifices in Fig. 4(b). The fundamental differences in streamline curvature properties of the uniform flow zone and the convergence can be seen in the figure. The curvature of streamlines in the flow through the single channel begins earlier upstream at $y/b \cong$ - 8 whereas in the flow through the adjacent orifices, the streamline curvature is seen mainly in the region -5 $\leq y/b \leq$5.

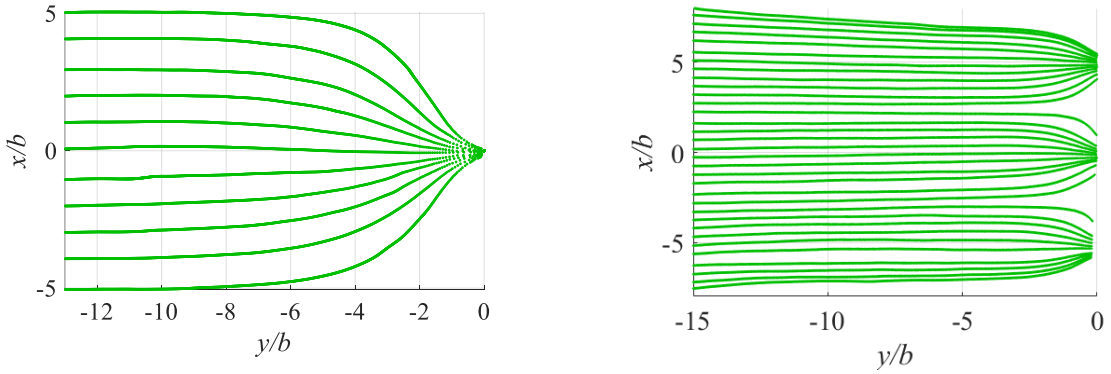

(a) (b)

Figure 4: Streamlines plotted for (a) a single orifice (b) multiple orifices

Pressure gradients along the streamlines were determined as per Eqs. (2) and (3). The plots in Fig. 5(a) show the pressure gradient for the section $0 \leq x/b \leq 5$ of the flow field in the single orifice case. The plots corresponding to the region of the central orifice ($0 \leq x/b \leq 2.5$) in the flow through multiple orifices are shown in Fig. 5(b). The center orifice is selected for a comparison between cases with difference in the wall boundaries in the upstream region. The upstream region in the single-orifice case is bounded by solid walls whereas the central orifice in the multiple orifices scenario has no solid walls leading to its entrance.

In both cases, the streamwise pressure gradient for $x/b = 0$ begins to increase to its maximum value earlier than other locations. From the plots it can also be seen that as the distance from the centerlines increases the increase in pressure drop begins at locations closer to the inlet of the channel.

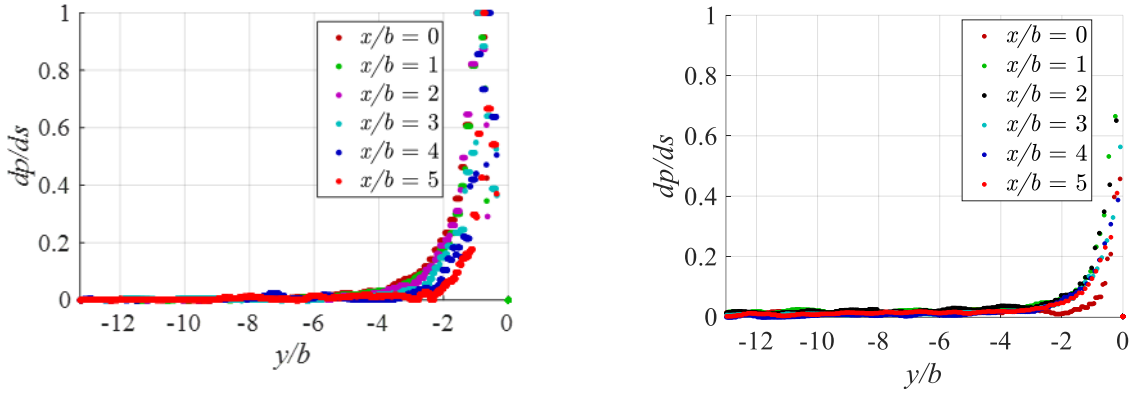

Figure 5: Streamwise pressure gradients for (a) a single orifice and (b) multiple orifices for *Re* = 0.1

The pressure gradient along the n- direction reflects the radius of curvature properties of the streamlines. The plots corresponding to the pressure gradient in the n-direction are given in Figure 6 for both cases of single orifice and multiple-orifices. In both cases, it can be seen that the as the curvature of the streamlines increase the pressure gradient in the n-direction increases. For the single orifice, the increase in the pressure gradient occurs closer to the inlet than for the case of multiple orifices.

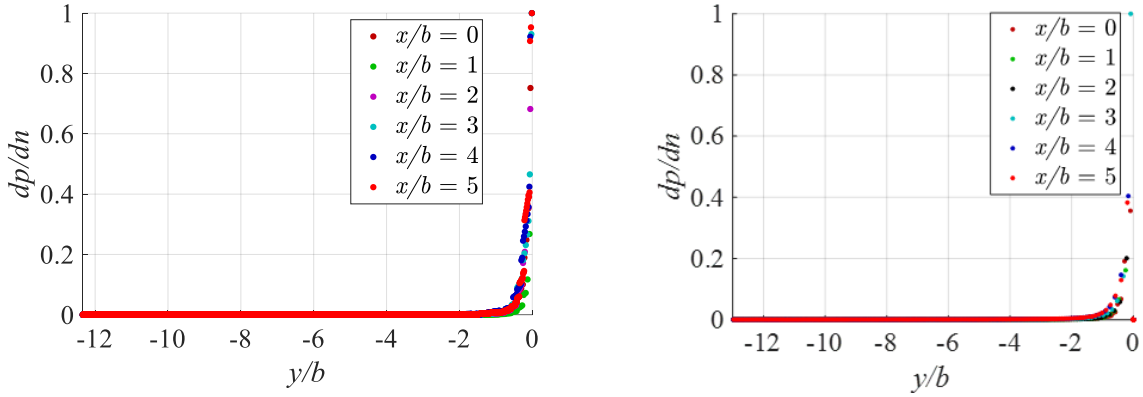

Figure 6: Pressure gradients in the n-direction in (a) single orifice (b) multiple orifices for Re = 0.1

For both cases, as *Re* increased the pressure gradients also increased due to the associated increase in the flow velocity. To identify the translation of this effect in terms of streamlines curvature, the

streamlines for $Re = 0.01$ and 0.1 are compared in Figure 7. It can be seen that for the flow at higher *Re*, the curvature of the streamlines is increased. The same behavior is also seen for the single orifice as reported in (Yusuf et al., 2018).

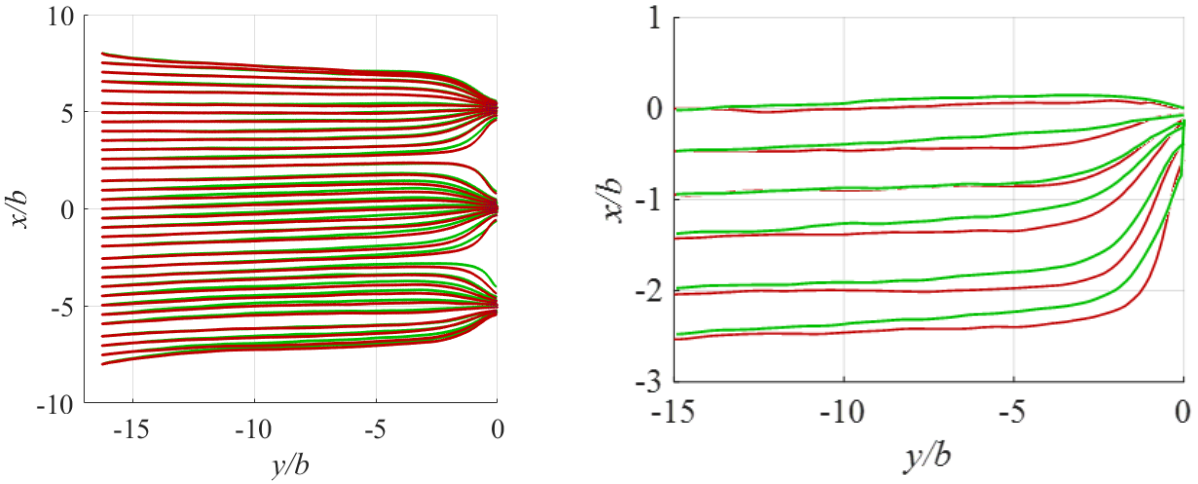

(a) (b)

Figure 7: Plots showing (a) streamlines for $\boldsymbol{Re} = 0.1$(red) and 0.01(green), with (b) a section of the flow field for a closer view at the streamline behavior for the different $\boldsymbol{Re}$ considered

Conclusion

The convergence phenomenon for the flow of glycerol entering single and multiple orifices is considered. The velocity field was measured with PSV experiments. The streamlines calculated from the processed vector field, were used to compare the curvature behavior as the flow enters the convergence zone. The pressure gradients in the streamwise and span-wise directions along the streamlines were determined using the equation of motion in streamline coordinates.

The results compared the cases for the single orifice and multiple orifice at $Re = 0.01$ and 0.1. The curvature of streamlines in the convergence region began earlier upstream for the case of the single orifice than the case of multiple orifices. The pressure gradients plots were also compared to show that the maximum increase in the streamwise gradient for the single-orifice, occurs farther from the inlet than in the case of multiple orifices. Comparing the pressure gradients in the n-direction showed a different relationship where the case of the single-orifice had the maximum increase closer to the inlet. The effect of *Re* on the curvature of streamlines in general conformed to what was observed in prior study where higher *Re* leads to higher curvature.

Acknowledgements

The authors gratefully acknowledge financial support from Natural Sciences and Engineering Research Council (NSERC) of Canada, the Alberta Ingenuity Fund, the Canadian Foundation for Innovation (CFI), and RGL Reservoir Management Inc.

References

Grose RD. (1983) Orifice flow at low Reynolds number. *Journal of Pipelines*, 3: 207–214.

Oliveira MSN, Alves MA, Pinho FT, and McKinley GH (2007) Viscous flow through microfabricated hyperbolic contractions. *Experiments in Fluids*, 43: 437-451.

Sonin AA (2010) Equation of Motion in Streamline Coordinates, Retrieved from http://mit.uvt.rnu.tn/NR/rdonlyres/Mechanical-Engineering/2-25Fall-2005/72039879-3550-4B1A-BCDC-3CD5CC519264/0/04_streamline.pdf

Utsunomiya T, Doshi R, Patel D, Mehta K, Nguyen D, Henry, WL, and Gardin JM (1993) Calculation of volume flow rate by the proximal isovelocity surface area method: Simplified approach using color Doppler zero baseline shift. *Journal of the American College of Cardiology*, 22: 277–282.

Yusuf Y, Baldygin A, Sabbagh R, Leitch M, Waghmare PR, and Nobes DS (2017a) Effect of Aspect Ratio on Pressure Loss and Characteristics of Low Reynolds Number Flow Through Narrow Slots. In *Proceedings of the 2nd Thermal and Fluid Engineering Conference, TFEC2017 4th International Workshop on Heat Transfer, IWHT2017*, *Las Vegas, Nevada, USA, April 4-7*.

Yusuf Y, Sabbagh R, and Nobes DS (2017b) Flow convergence model for flow through long aspect ratio rectangular orifices. In *Okanagan Fluid Dynamics Meeting, Kelowna, British Columbia, Canada, August 21-24,*

Yusuf Y, Ansari S, Bayans M, Sabbagh R, Hassan MEl, and Nobes DS (2018) Study of Flow Convergence in Rectangular Slots using Particle Shadowgraph Velocimetry. In *Proceedings of the 5th International Conference on Experimental Fluid Mechanics – ICEFM 2018 Munich, Munich, Germany, July 2-4*.

Yusuf Y, Sabbagh R, and Nobes DS (2019) Semi-empirical pressure loss model for viscous flow through rectangular orifices. *Physics of Fluids*, 1-38 (under 3rd revision)